Articles

Isolation and Structural Characterization of Tetra-*n*-propyl Zirconate in Hydrocarbon Solution and the Solid State

Victor W. Day,*,† Walter G. Klemperer,*,‡ and Margaret Mary Pafford‡

Department of Chemistry, University of Nebraska, Lincoln, Nebraska 68588, and Department of Chemistry, University of Illinois, Urbana, Illinois 61801

Received July 20, 2001

Tetra-*n*-propyl zirconate has been purified by vacuum distillation and isolated as an extremely moisture sensitive, crystalline solid. According to a single-crystal X-ray diffraction study, crystalline tetra-*n*-propyl zirconate is composed of tetrameric $Zr_4(OPr^n)_{16}$ (**1**) molecules whose Zr_4O_{16} metal−oxygen core structure has virtual C_{2h} symmetry, the same structure observed previously for *n*-alkyl orthotitanates. Carbon-13 NMR spectroscopic data indicate that this core structure is retained in hydrocarbon solution. Molecule **1** has the same M_4O_{16} metal−oxygen core structure as $[CH_3C(CH_2O)_3]_2M_4(OPr^i)_{10}$, M = Ti, where the metal centers have octahedral coordination geometry, but a metal−oxygen core structure different from that of the M = Zr case, where trigonal metaprismatic coordination geometry is observed.

Introduction

The utility[1,2] of *n*-alkyl orthozirconates $Zr(Oalkyl^n)_4$ derives in part from their facile conversion to zirconium oxide according to reaction 1.[8−10] This reaction has the chain mechanism

$$Zr(Oalkyl^n)_4 \rightarrow ZrO_2 + 2\ n\text{-alkene} + 2\ n\text{-alcohol} \quad (1)$$

$$Zr{-}Oalkyl^n + BH \rightarrow Zr{-}B + n\text{-alcohol} \quad (2)$$

$$n\text{-alcohol} \rightarrow n\text{-alkene} + H_2O \quad (3)$$

$$2\ Zr{-}Oalkyl^n + H_2O \rightarrow Zr{-}O{-}Zr + 2\ n\text{-alcohol} \quad (4)$$

indicated in reactions 2−4, and zirconium alkoxide decomposition can be induced by trace amounts of a Brønsted acid initiator, BH, usually water, alcohol, or glass surface hydroxyl groups.[8,9] Homoleptic zirconium(IV) *n*-alkoxides and other homoleptic zirconium(IV) alkoxides containing β-hydrogen atoms are therefore extremely difficult to purify and have to date not been isolated in pure form.[11−14] As a result, the reaction chemistry of these "simple" zirconium alkoxides, believed to be quite different from the chemistry of their silicon and titanium analogues, is poorly understood.[15−18] We report here the isolation of tetra-*n*-propyl zirconate in pure, crystalline form and the determination of its molecular structure both in solution and in the solid state.

† University of Nebraska.
‡ University of Illinois.

(1) Commercial applications of *n*-propyl zirconate (Tyzor NPZ) and *n*-butyl zirconate (Tyzor NBZ) include catalysis, surface modification, cross-linking, and adhesion promotion. See http://www.dupont.com/tyzor/.
(2) Other areas of application involving zirconium *n*-alkoxides include integrated optical waveguides,[3] mesostructured materials,[4] chemical vapor deposition,[5] synthesis of mixed-metal perovskite materials,[6] and preparation of heterogeneous catalysts including sulfated zirconia.[7]
(3) (a) Urlacher, C.; Dumas, J.; Serughetti, J.; Mugnier, J.; Munoz, M. *J. Sol-Gel Sci. Technol.* **1997**, *8*, 999−1005. (b) Sorek, Y.; Zevin, M.; Reisfeld, R.; Hurvits, T.; Rushin, S. *Chem. Mater.* **1997**, *9*, 670−676. (c) Schmidt, H. K.; Krug, H.; Zeitz, B.; Geiter, E. *Proc. SPIE-Int. Soc. Opt. Eng.* **1997**, *3136*, 220−228. (d) Coudray, P.; Etienne, P.; Porque, J.; Moreau, Y.; Najafi, S. I. *Proc. SPIE-Int. Soc. Opt. Eng.* **1998**, *3278*, 252−258.
(4) (a) Liu, P.; Reddy, J. S.; Adnot, A.; Sayari, A. *Mater. Res. Soc. Symp. Proc.* **1996**, *431*, 101−110. (b) Pacheco, G.; Zhao, E.; Garcia, A.; Sklyarov, A.; Fripiat, J. J. *Chem. Commun.* **1997**, 491−492. (c) Wong, M. S.; Ying, J. Y. *Chem. Mater.* **1998**, *10*, 2067−2077. (d) Ciesla, U.; Froeba, M.; Stucky, G.; Schueth, F. *Chem. Mater.* **1999**, *11*, 227−234.
(5) (a) Bradley, D. C. *Chem. Rev.* **1989**, *89*, 1317−1322. (b) Nakamura, S.; Yoshishige, H.; Eiji, H. *Kagaku Kogaku Ronbunshu* **1990**, *16*, 490−493. (c) Xue, Z.; Vaartstra, B. A.; Caulton, K. G.; Chisholm, M. H.; Jones, D. L. *Eur. J. Solid State Inorg. Chem.* **1992**, *29*, 213−225. (d) Nakamura, S.; Hayashi, Y.; Kawanishi, T.; Gotoh, K. *Kagaku Kogaku Ronbunshu* **1994**, *20*, 648−656.
(6) Chandler, C. D.; Roger, C.; Hampden-Smith, M. J. *Chem. Rev.* **1993**, *93*, 1205−1241.
(7) (a) Inoue, M.; Kominami, H.; Inui, T. *Appl. Catal., A* **1993**, *97*, L25-L30. (b) Ward, D. A.; Ko, E. I. *Chem. Mater.* **1993**, *5*, 956−969. (c) Inoue, M.; Kominami, H.; Inui, T. *Res. Chem. Intermed.* **1998**, *24*, 571−579. (d) Armendariz, H.; Coq, B.; Tichit, D.; Dutartre, R.; Figueras, F. *J. Catal.* **1998**, *173*, 345−354.
(8) Bradley, D. C.; Faktor, M. M. *Trans. Faraday Soc.* **1959**, *55*, 2117−2123.
(9) Bradley, D. C.; Faktor, M. M. *J. Appl. Chem.* **1959**, *9*, 435−439.
(10) Mazdiyasni, K. S.; Lynch, C. T.; Smith, J. S. *J. Am. Ceram. Soc.* **1965**, *48*, 372−375.
(11) Bradley, D. C.; Wardlaw, W. *J. Chem. Soc.* **1951**, 280−285.
(12) Bradley, D. C.; Mehrotra, R. C.; Swanwick, J. D.; Wardlaw, W. *J. Chem. Soc.* **1953**, 2025−2030.
(13) Turevskaya, E. P.; Kozlova, N. I.; Belokon, A. I.; Berdyev, D. V.; Kessler, V. G.; Grishin, Y. K. *Russ. Chem. Bull.* **1995**, *44*, 734−742.
(14) Turova, N. Y.; Turevskaya, E. P.; Yanovskaya, M. I.; Yanovsky, A. I.; Kessler, V. G.; Tcheboukov, D. E. *Polyhedon* **1998**, *17*, 899−915.
(15) Hubert-Pfalzgraf, L. G. *New J. Chem.* **1987**, *11*, 663−675.
(16) Livage, J.; Henry, M.; Sanchez, C. *Prog. Solid State Chem.* **1988**, *18*, 259−341.
(17) Sanchez, C.; Livage, J. *New J. Chem.* **1990**, *14*, 513−521.
(18) Livage, J. In *Encyclopedia of Inorganic Chemistry*; King, R. B., Ed.; Wiley: New York, 1994; Vol. 7, pp 3836−3851.

10.1021/ic010776g CCC: $20.00
Published on Web 10/29/2001

The detailed structural analysis reported here was motivated by a recent report on the synthesis and crystal structures of two tetranuclear, tetravalent metal alkoxides, $[CH_3C(CH_2O)_3]_2M_4(OPr^i)_{10}$, M = Ti and Zr.[19] These molecules are remarkable by virtue of their different metal−oxygen core structures. The titanium compound has the M_4O_{16} metal−oxygen core structure shown in **a**,[20] where spheres representing oxygen atoms from

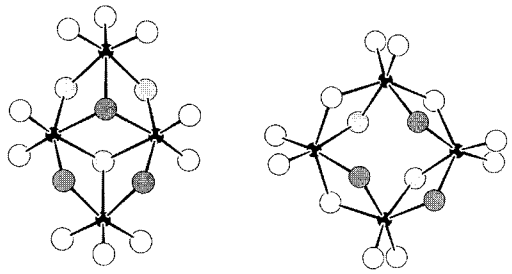

a **b**

the same tridentate chelate ligands are similarly shaded. This structure is also observed in the solid state for the tetrameric orthotitanates $Ti_4(OCH_2CH_3)_{16}$,[21] $Ti_4(OCH_3)_4(OCH_2CH_3)_{12}$,[22] $Ti_4(OCH_3)_{16}$,[23] $[CH_3C(CH_2O)_3]_2Ti_4(OPr^i)_{10}$,[19] and $[CH_3CH_2C(CH_2O)_3]_2Ti_4(OPr^i)_{10}$.[19] Unlike the orthotitanates, $[CH_3C(CH_2O)_3]_2Zr_4(OPr^i)_{10}$ adopts the metal−oxygen core structure shown in **b**,[2] where spheres representing oxygen atoms from the tridentate chelate ligands are shaded as in **a**. This structure has been reported for the Mo_4O_{16} core of $[Mo_4O_{12}(O_2)_2]^{4-}$ [24,25] and the $Ti_4F_8N_8$ core of $[(Me_2N)_2TiF_2]_4$.[26] Structures **a** and **b** differ in three respects. First, the metal centers in **a** form a diamond, but the metal centers in **b** form a square. Second, the metal centers in **a** have approximately octahedral coordination geometry, whereas the metal centers in structure **b** have coordination geometry distorted from octahedral toward trigonal prismatic; that is, they adopt trigonal metaprismatic[27] coordination geometry. Third, structures **a** and **b** have different distributions of triply bridging (μ_3), doubly bridging (μ_2), and terminal (t) oxygen ligands, namely, $M_4(\mu_3\text{-}O)_2(\mu_2\text{-}O)_4(O_t)_{10}$ and $M_4(\mu_2\text{-}O)_8(O_t)_8$, respectively. We were therefore curious to determine whether tetra-*n*-propyl zirconate would adopt metal−oxygen core structure **a** or **b**, or perhaps a different $(MO_4)_n$ metal−oxygen core structure.[28]

Experimental Section

Reagents, Solvents, and General Procedures. Tetra-*n*-propyl zirconate, 70% solution by weight in 1-propanol, was purchased fromAldrich Chemical Co., Inc. Molecular sieves (3 Å Linde type A, Grace Davison) were activated by heating at 250 °C for at least 24 h and cooling under vacuum. HPLC grade *n*-heptane (Fisher Scientific), HPLC grade *n*-pentane (Fisher Scientific), methylcyclohexane (Aldrich), and toluene (Fisher Scientific) were dried over activated molecular sieves, refluxed over Na, and freshly distilled before use. Diethyl ether (Fisher Scientific) and benzene (Fisher Scientific) were dried over activated molecular sieves, refluxed over Na/benzophenone, and freshly distilled before use. Cyclohexane-d_{12} (Cambridge Isotope Laboratories) was dried over activated molecular sieves for at least 24 h and subsequently distilled. Methylcyclohexane-d_{14} (Cambridge Isotope Laboratories) was dried over Na/K alloy for 24 h, degassed using three freeze−pump−thaw cycles, and distilled from Na/K alloy. All other solvents were dried over activated molecular sieves for at least 24 h.

Tetra-*n*-propyl zirconate is an extremely moisture sensitive material, and all manipulations were carried out under an argon or nitrogen atmosphere using standard Schlenk and drybox techniques. All glassware was washed in an ethanolic KOH bath, rinsed with dilute HCl, rinsed with deionized water, and oven-dried for 12 h at 120 °C. Finally, the glassware was thoroughly flame-dried before use by passing the flame from a Bunsen burner over the entire surface of the flask under vacuum (ca. 10^{-2} mmHg). Water vapor was observed on the surface of the flask upon contact of the flame with the glass, and the glassware was heated for approximately 3 min until no further water vapor was visible. The flask was then allowed to cool under vacuum.

Analytical Procedures. Both 500 MHz ^{1}H and 125.6 MHz ^{13}C-{^{1}H} NMR spectra were measured on a Varian Unity 500 spectrometer, and those recorded at 750 and 188.6 MHz, respectively, were measured on a Varian Unity Inova 750 spectrometer. Gradient-enhanced ^{1}H−^{1}H COSY experiments, gradient phase-sensitive ^{1}H−^{13}C heteronuclear multiple-quantum coherence (HMQC) experiments, and ^{13}C inversion−recovery experiments were performed using standard pulse programs.[35] Chemical shifts were internally referenced to tetramethylsilane (δ = 0.00). NMR samples were typically prepared by distilling 0.75 mL of deuterated solvent into a 5 mm o.d. NMR sample tube containing ca. 45 mg of tetra-*n*-propyl zirconate. The tube was then flame-sealed under vacuum. Elemental analysis was performed by the University of Illinois Microanalytical Service Laboratory.

Isolation and Purification of Zr(OPr^n)$_4$. A 250 mL, two-neck, round bottom flask with ground-glass joints was charged with 100 mL of a 70 wt % solution of partially hydrolyzed tetra-*n*-propyl zirconate in 1-propanol. The flask was then joined to a nitrogen inlet and a distillation apparatus constructed from a 24 mm i.d. Vigreux reflux column 20.3 cm in length, a distillation head with a thermometer, and a Liebig condenser with a jacket length of 20.0 cm. The components of the distillation apparatus were not connected by ground-glass joints but were instead integrated into a single piece of glassware. A 100 mL, single-neck, receiving flask was joined to the still body by an elbow fitted with a nitrogen/vacuum inlet. All ground-glass joints were sealed with silicone grease and secured with copper wire. 1-Propanol was removed from the partially hydrolyzed tetra-*n*-propyl zirconate solution under nitrogen by heating the distillation flask in a silicone oil heating bath and collecting all material that distilled at temperatures of less than 100 °C at ambient pressure. The waxy yellow solid remaining in the distillation flask was allowed to cool to room temperature.

(19) Boyle, T. J.; Schwartz, R. W.; Doedens, R. J.; Ziller, J. W. *Inorg. Chem.* **1995**, *34*, 1110−1120.
(20) In **a** and **b**, the M_4O_{16} structures[19] are shown in projection onto the M_4 plane.
(21) Ibers, J. *Nature* **1963**, *197*, 686−687.
(22) Witters, R. D.; Caughlan, C. N. *Nature* **1965**, *205*, 1312−1313.
(23) Wright, D. A.; Williams, D. A. *Acta Crystallogr.* **1968**, *B24*, 1107−1114.
(24) Stomberg, R.; Trysberg, L.; Larking, I. *Acta Chem. Scand.* **1970**, *24*, 2678−2679.
(25) Olson, S.; Stomberg, R. *Z. Kristallogr.* **1996**, *211*, 895−899.
(26) Sheldrick, W. S. *J. Fluorine Chem.* **1974**, *4*, 415−421.
(27) O'Keeffe, M.; Hyde, B. G. *Crystal Structures I. Patterns and Symmetry*; Mineralogical Society of America: Washington, DC, 1996; p 140.
(28) In the solid state, barium orthotitanates[29] are monomeric; tetraneopentyl orthotitanate,[30a] tetraneopentyl orthozirconate,[30b] and Ti(2,4-dimethyl-2,4-pentanediolate)$_2$[31] are dimeric with $M_2(\mu_2\text{-}O)_2(O_t)_6$ core structures; alkyl titanocarboxylates have $Ti_4(\mu_3\text{-}O)_4(O_t)_{12}$ core structures in $Ti_4O_4(OR)_4(O_2CR')_4$ (R = *t*-Bu, R′ = *i*-Pr;[32] R = *i*-Pr or Ph, R′ = $CCo_3(CO)_9$[33]) and $Ti_4(\mu_4\text{-}O)(\mu_2\text{-}O)_5(O_t)_{10}$ core structures in $Ti_4O_2(OR)_{10}(O_2CR')_2$ (R = Et, R′ = adamantyl[32]); and strontium orthotitanate[34] has a polymeric, perovskite-like $[Ti(\mu_2\text{-}O)_{4/2}(O_t)_2]_\infty$ titanium−oxygen core structure.
(29) (a) Günter, J. R. *Acta Crystallogr.* **1984**, *C40*, 207−210. (b) Wu, K. K.; Brown, I. D. *Acta Crystallogr.* **1973**, *B29*, 2009−2012.
(30) (a) Boyle, T. J.; Alam, T. M.; Mechenbier, E. R.; Scott, B. L.; Ziller, J. W. *Inorg. Chem.* **1997**, *36*, 3292−3300. (b) Boyle, T. J. (Sandia National Laboratories). Personal communication, 1999.
(31) Damo, S. M.; Lam, K.-C.; Rheingold, A.; Walter, M. A. *Inorg. Chem.* **2000**, *39*, 1635−1638.
(32) Charnick, S.; Day, V. D.; Klemperer, W. G. Manuscript in preparation.
(33) Lei, X. J.; Shang, M. Y.; Fehlner, T. P. *Organometallics* **1996**, *15*, 3779−3781.
(34) Tilley, R. J. D. *J. Solid State Chem.* **1977**, *21*, 293−301.
(35) System Operation, VNMR Version 5.1 Software, Varian Associates, Inc., Nuclear Magnetic Resonance Instruments, Palo Alto, CA, 1995.

Tetra-*n*-propyl zirconate was distilled under vacuum from the same distillation flask used for solvent removal but using a different distillation apparatus suited for higher temperatures and lower pressures. A 40 wt % $NaNO_2$, 7 wt % $NaNO_3$, and 53 wt % KNO_3 heating bath[36] was employed. The distillation flask was fitted with a still body identical to the one described above except that the Liebig condenser was replaced with a simple, 1.25 cm i.d. glass condenser. A cow receiver equipped with a nitrogen/vacuum inlet and fitted with one 50 mL and two 100 mL Schlenk flask receivers spaced 45° apart was attached to the still body. All ground-glass joints were sealed with Krytox LVP fluorinated grease (70% perfluoroalkyl ether, 30% poly(tetrafluoroethylene)) and secured with copper wiring. A thermocouple probe was attached to the surface of the condenser, which was subsequently wrapped with heating tape insulated with braided fibrous glass, and the still body and condenser were heavily insulated with glass wool and aluminum foil. The system was evacuated to ca. 10^{-2} mmHg of pressure, the condenser was heated to ca. 175 °C, and finally, the temperature of the heating bath was raised to 290 °C. Three distinct distillation fractions were observed as the temperature at the distillation head was allowed to rise to 270 °C, and these three fractions were collected as follows. Less than 3 mL of a yellow oil distilled at 185−220 °C, the precise amount depending upon the purity of the crude material. About 40 g of analytically pure (see below) tetra-*n*-propyl zirconate was collected between 225 and 245 °C as a clear, colorless liquid that solidified immediately upon contact with the collection flask. Finally, about 10 g of a third fraction was collected between 250 and 270 °C as a waxy white or slightly yellow solid. About 20 g of the crude material remained in the distillation pot. *Extreme caution was exercised to maintain the condenser at an elevated temperature throughout the distillation, because solidification of the distillate in the condenser at lower temperatures would generate a closed and hence extremely hazardous system*.

During the course of optimizing the procedures just described, timing was found to be critically important. Specifically, material in the distillation pot could not be raised to temperatures above about 200 °C for longer than about 40 min. If the distillation was carried out more slowly, a distinct second distillation fraction was not observed, and the tetra-*n*-propyl zirconate collected at elevated distillation temperatures was seriously contaminated.

Tetra-*n*-propyl zirconate is highly soluble in diethyl ether, 1-propanol, toluene, benzene, methylene chloride, 1,2-dichloroethane, and hydrocarbons such as *n*-heptane, *n*-pentane, and methylcyclohexane. It can be crystallized from *n*-heptane, *n*-pentane, toluene, methylene chloride, and 1,2-dichloroethane as described below. Crystallization does not generally improve the purity of the distilled $Zr(OPr^n)_4$. Quite to the contrary, repeated recrystallizations generally yielded increasingly impure material, presumably because of its extreme moisture sensitivity. Anal. Calcd for $Zr_4O_{16}C_{48}H_{112}$ C, 44.00; H, 8.62; Zr, 27.85. Found: C, 43.68; H, 8.87; Zr, 28.33. ^{1}H NMR (500 MHz, cyclohexane-d_{12}, 22 °C): δ 4.20−3.90 (16H, m, $-OCH_2CH_2CH_3$), 2.13 (2H, br sext, J = 7.7 Hz, $-OCH_2CH_2CH_3$), 1.90 (2H, br m, $-OCH_2CH_2CH_3$), 1.80 (2H, br m, $-OCH_2CH_2CH_3$), 1.67 (4H, sext, J = 7.4 Hz, $-OCH_2CH_2CH_3$), 1.60 (6H, br m, $-OCH_2CH_2CH_3$), 0.94 (9H, t, J = 7.4 Hz, $-OCH_2CH_2CH_3$), 0.90 (6H, t, J = 7.5 Hz, $-OCH_2CH_2CH_3$), 0.86 (6H, t, J = 7.6 Hz, $-OCH_2CH_2CH_3$), 0.83 (3H, t, J = 7.5 Hz, $-OCH_2CH_2CH_3$). ^{1}H NMR (750 MHz, methylcyclohexane-d_{14}, −20 °C): δ 3.91−4.15 (16H, m, $-OCH_2CH_2CH_3$), 2.12 (2H, br sext, $-OCH_2CH_2CH_3$), 1.89 (2H, br m, $-OCH_2CH_2CH_3$), 1.78 (2H, br m, $-OCH_2CH_2CH_3$), 1.66 (4H, sext, J = 7.3 Hz, $-OCH_2CH_2CH_3$), 1.59 (4H, sext, J = 7.3 Hz, $-OCH_2CH_2CH_3$), 1.58 (2H, sext, J = 7.3 Hz, $-OCH_2CH_2CH_3$), 0.95 (6H, t, J = 7.3 Hz, $-OCH_2CH_2CH_3$), 0.94 (3H, t, J = 7.3 Hz, $-OCH_2CH_2CH_3$), 0.90 (6H, t, J = 7.3 Hz, $-OCH_2CH_2CH_3$), 0.87 (6H, t, J = 7.3 Hz, $-OCH_2CH_2CH_3$), 0.83 (3H, t, J = 7.3 Hz, $-OCH_2CH_2CH_3$). ^{13}C{^{1}H} NMR (125.6 MHz, cyclohexane-d_{12}, 22 °C): δ 73.55 (1C, $-OCH_2CH_2CH_3$), 73.49 (2C, $-OCH_2CH_2CH_3$), 73.25 (2C, $-OCH_2CH_2CH_3$), 72.41 (3C, $-OCH_2CH_2CH_3$), 28.86 (2C, $-OCH_2CH_2CH_3$), 28.47 (1C, $-OCH_2CH_2CH_3$), 27.92 (2C, $-OCH_2CH_2CH_3$), 26.85 (2C, $-OCH_2CH_2CH_3$), 24.30 (1C, $-OCH_2CH_2CH_3$), 10.96 (3C, $-OCH_2CH_2CH_3$), 10.60 (2C, $-OCH_2CH_2CH_3$), 10.19 (1C, $-OCH_2CH_2CH_3$), 10.00 (2C, $-OCH_2CH_2CH_3$). ^{13}C{^{1}H} NMR (188.6 MHz, methylcyclohexane-d_{14}, −20 °C): δ 73.28 ($-OCH_2CH_2CH_3$), 73.13 ($-OCH_2CH_2CH_3$), 73.06 ($-OCH_2CH_2CH_3$), 72.07 ($-OCH_2CH_2CH_3$), 72.03 ($-OCH_2CH_2CH_3$), 28.68 ($-OCH_2CH_2CH_3$), 28.27 ($-OCH_2CH_2CH_3$), 27.74 ($-OCH_2CH_2CH_3$), 26.70 ($-OCH_2CH_2CH_3$), 23.96 ($-OCH_2CH_2CH_3$), 11.03 ($-OCH_2CH_2CH_3$), 11.01 ($-OCH_2CH_2CH_3$), 10.64 ($-OCH_2CH_2CH_3$), 10.39 ($-OCH_2CH_2CH_3$), 10.14 ($-OCH_2CH_2CH_3$).

X-ray Crystallographic Study of $Zr(OPr^n)_4$. Single crystals of tetra-*n*-propyl zirconate were grown from 1,2-dichloroethane solution by adding 1,2-dichloroethane in 50 μL increments at 80 °C in a silicone oil bath until all of the alkoxide was dissolved; about 450 μL of 1,2-dichloroethane was added for a 1 g sample. The solution was cooled to room temperature over the course of about 1 h, and clear, colorless, tabular crystals formed within about 3 h. Single crystals were removed from the mother liquor in an inert atmosphere and mounted for data collection with mother liquor present in a 0.7 mm i.d. glass capillary (0.01 mm walls, Glas Berlin-West, distributed by Charles Supper Co.) sealed with epoxy.

Tetra-*n*-propyl zirconate forms molecular $Zr_4(OCH_2CH_2CH_3)_{16}$ crystals that are triclinic at 20 ± 2 °C, space group $P\bar{1}$-C_i^1 (no. 2) with a = 12.115(1) Å, b = 12.675(1) Å, c = 13.869(1) Å, α = 64.369(2)°, β = 81.369(3)°, γ = 67.737(3)°, V = 1776.7(3) Å^3, and Z = 1, tetranuclear molecule [d_{calcd} = 1.225 g cm^{-3}; μ_a(Mo Kα) = 0.62 mm^{-1}]. Since crystals frequently shattered upon cooling below room temperature, the data were collected at ambient temperature. A full hemisphere of diffraction intensities (ω scan width of 0.50°) was measured using graphite-monochromated Mo Kα radiation on a Bruker SMART CCD single-crystal diffraction system.[37] X-rays were provided by a normal-focus sealed X-ray tube operated at 50 kV and 40 mA. Lattice constants were determined with the Bruker SAINT software package using peak centers for 2078 reflections. A total of 5833 integrated reflection intensities having 2θ(Mo Kα) < 45.0° were produced using the Bruker program SAINT.[38] A total of 4049 of these were independent and gave R_{int} = 0.060. The structure was solved and refined using the Bruker SHELXTL-PC Version 5 software package.[39] Structure solution was accomplished using "direct methods" techniques, and all stages of weighted full-matrix least-squares refinement were conducted using F_o^2 data. Final agreement factors at convergence were R1 (unweighted, based on F) = 0.097 for 2228 independent absorption-corrected reflections having 2θ(Mo Kα) < 45.0° and $I > 2\sigma(I)$ and wR2 (weighted, based on F^2) = 0.258 for 3234 independent absorption-corrected reflections having 2θ(Mo Kα) < 45.0° and $I > 0$. Final agreement factors for all of the data were P_1 (unweighted, based on F) = 0.160 and wR2 (weighted, based on F^2) = 0.339 for all 4049 independent absorption-corrected reflections having 2θ(Mo Kα) < 45.0°. The crystallographic data are summarized in Table 1.

The structural model employed incorporated anisotropic thermal parameters for all non-hydrogen atoms and isotropic thermal parameters for all hydrogen atoms. Six of the eight crystallographically independent propyl groups were disordered in the lattice. All six of these groups had alternate positions for one of their methylene carbons, and in addition, one of these propyl groups had alternate positions for its methyl carbon. Normalized occupancy factors for these disordered carbons were assigned by varying the relative occupancies to give nearly equal equivalent isotropic thermal parameters for both positions. The U_{ij} components of the anisotropic thermal parameters for all 14 of the partial-occupancy carbon atoms and 2 full-occupancy methyl carbon atoms were restrained with an estimated standard deviation of 0.02−

(36) Gordon, A. J.; Ford, R. A. *The Chemists's Companion, A Handbook of Practical Data, Techniques, and References*; Wiley: New York, 1972; pp 449−450.

(37) SMART Software Reference Manual, Data Collection Software for CCD and Multiwire Area Detectors, Siemens Industrial Automation, Inc., Madison, WI, 1994.

(38) SAINT Version 4 Software Reference Manual, Data Reduction Software for Single-Crystal Diffraction with an Area Detector, Siemens Analytical Instruments, Inc., Madison, WI, 1995.

(39) SHELXTL Version 5 Reference Manual, Crystal Structure Solution and Refinement Software, Siemens Analytical X-Ray Instruments, Inc., Madison, WI, 1994.

Table 1. Crystal Data and Structure Refinement for $Zr_4(OPr^n)_{16}$

empirical formula	$C_{48}H_{112}O_{16}Zr_4$
fw	1310.24
temp	293(2) K
wavelength	0.71073 Å
crystal system	triclinic
space group	$P\bar{1}$-C_i^1 (No. 2)
unit cell dimensions	$a = 12.115(1)$ Å, $\alpha = 64.369(2)°$
	$b = 12.675(1)$ Å, $\beta = 81.369(3)°$
	$c = 13.869(1)$ Å, $\gamma = 67.737(3)°$
volume, Z	1776.7(3) Å^3, 1 tetranuclear unit
density(calcd)	1.225 g/cm^3
absorption coefficient	0.620 mm^{-1}
$F(000)$	688
crystal size	0.62 × 0.48 × 0.40 mm
θ range for data collection	1.63−22.50°
limiting indices	$-14 \le h \le 14$
	$-14 \le k \le 15$
	$-5 \le l \le 16$
reflections collected	5833
independent reflections	4049 [$R_{int} = 0.060$]
absorption correction	semiempirical from ψ-scans
max and min transmission	0.8458 and 0.6622
refinement method	full-matrix least-squares on F^2
no. of data/restraints/params	3234/157/372
goodness-of-fit on F^2	1.099
final R indices [$I > 2\sigma(I)$]	$R_1{}^a = 0.097$, $wR_2{}^b = 0.235$
R indices (all data)	$R_1{}^a = 0.160$, $wR_2{}^b = 0.339$
largest diff peak and hole	0.410 and −0.255 e$^-$/Å^3

^{a} $R_1 = \sum||F_o| - |F_c||/\sum|F_o|$. ^{b} $wR_2 = [\sum[w(F_o^2 - F_c^2)^2]/\sum[w(F_o^2)^2]]^{1/2}$.

0.2 to approximate isotropic behavior. The zirconium and oxygen atoms all appeared to be ordered.

Hydrogen atoms were included in the structural model at idealized positions, assuming approximate (methylene) and rigorous (methyl) sp^3-hybridization of carbon atoms and C−H bond lengths of 0.97 and 0.96 Å for methylene and methyl groups, respectively. The isotropic thermal parameters of these idealized hydrogen atoms were fixed at values 1.2 (methylene) or 1.5 (methyl) times the equivalent isotropic thermal parameter of the carbon atom to which they are covalently bonded. The O−C and C−C bond lengths for the disordered *n*-propoxide ligands were restrained to have common values which were included as free variables in the least-squares refinement; the final refined values were 1.46(1) and 1.47(2) Å, respectively. The O−C_α–C_β and C_α–C_β–C_γ angles for the disordered ligands were restrained to nearly tetrahedral values by requiring the O···C_β and C_α···C_γ separations to be within 0.2 Å of the distance implied by 109.5° O−C_α–C_β and C_α–C_β–C_γ angles. No restraints were applied to the parameters of the metal oxide core or the ordered B-type μ_2-bonded ligands. Selected average interatomic distances are given with estimated standard deviations in Table 2.

Results

Isolation of $Zr(OPr^n)_4$. Solvent was removed from a commercially available, 70 wt % solution of tetra-*n*-propyl zirconate in 1-propanol by distillation at 85−98 °C under N_2 at ambient pressure, and the waxy solid thus obtained was then fractionally distilled under N_2 at ca. 10^{-2} mmHg of pressure. A 225−245 °C fraction was collected as a clear, colorless liquid that solidified upon contact with the receiving flask, yielding analytically pure $Zr(OPr^n)_4$. Tetra-*n*-propyl zirconate is most conveniently identified by ^{1}H NMR spectroscopy in cyclohexane-d_{12} solution at ambient temperature: four triplets are observed in the methyl proton region at δ 0.94, 0.90, 0.86, and 0.83 with relative intensities of 3:2:2:1. Low-intensity ^{1}H NMR triplets observed at δ 0.93 and 0.92 arise from an impurity, the hydrolysis product $Zr_3O(OPr^n)_{10}$,[14] a material that can be prepared in high yield under controlled conditions.[40] Tetra-*n*-propyl zirconate is an extremely moisture sensitive material. As a result, NMR samples were almost invariably contaminated with 1−3% of this impurity and elemental analyses were generally slightly higher than their calculated values for zirconium and slightly lower than their calculated values for carbon. Extraordinary measures were not taken to dehydrate/dehydroxylate glass surfaces, however, beyond flame-drying the glassware under vacuum.

(40) Klemperer, W. G.; Pafford, M. M. Manuscript in preparation.

Table 2. Comparison of Selected Bond Lengths and O···O Polyhedral Edge Lengths Involving the M_4O_{16} Cores in Crystalline $Zr_4(OPr^n)_{16}$ (**1**), $[CH_3C(CH_2O)_3]_2Ti_4[[OCH(CH_3)_2]_{10}$ (**2**), and $[CH_3CH_2C(CH_2O)_3]_2Ti_4[[OCH(CH_3)_2]_{10}$ (**3**)

	average value[41]		
type[a]	M = Zr (**1**)	M = Ti (**2, 3**)	difference Δ
	Metal−Oxygen Bond Lengths, Å		
M1−OA	2.32(1,1,1,2)	2.180(3,25,32,4)	0.14 (6%)
M1−OB	2.11(1,4,4,2)	1.966(3,16,20,4)	0.14 (7%)
M1−OC	1.92(1,1,1,2)	1.790(3,21,28,4)	0.13 (7%)
M2−OA	2.35(1)	2.230(3,3,3,2)	0.12 (5%)
M2−OB	2.24(1,1,1,2)	2.119(3,25,30,4)	0.12 (6%)
M2-OD	1.96(1,1,1,2)	1.812(3,21,28,4)	0.15 (8%)
M2−OE	1.93(1)	1.825(3,4,4,2)	0.10 (6%)
	O···O Octahedral Edge Lengths, Å		
M1 O···O	2.97	2.773	0.20 (7%)
M2 O···O	2.95	2.772	0.18 (6%)
	M···M Separations, Å		
M1···M2	3.624(2,0,0,2)	3.334(1,10,17,4)	0.29 (9%)
M1···M1′	3.678(3)	3.477(1,2,2,2)	0.20 (6%)
M2···M2′	6.245(3)	5.690(1,5,5,2)	0.56 (10%)

[a] Atoms labeled as in Figures 1 and 4. Atoms in all three molecules labeled with a prime are related to those labeled without a prime by a crystallographic inversion center located at the center of the molecule.

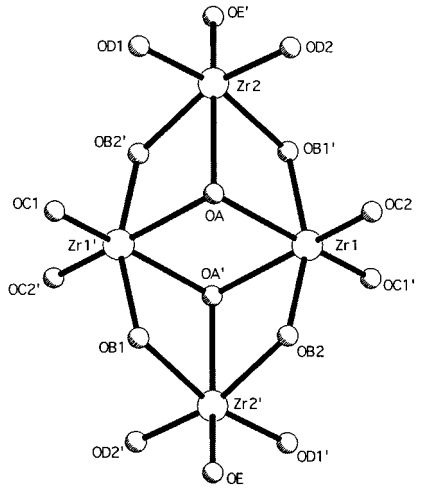

Figure 1. Zr_4O_{16} metal−oxygen core structure of the $Zr_4(OPr^n)_{16}$ molecule. Zirconium and oxygen atoms are represented by large and small spheres, respectively.

Solid-State Structure. According to a single-crystal X-ray diffraction study, tetra-*n*-propyl zirconate is a tetramer in the solid state. The crystallographically centrosymmetric Zr_4O_{16} core structure of $Zr_4(OPr^n)_{16}$ (**1**) is shown in Figure 1, and selected interatomic distances are provided in Table 2. As indicated in Figure 1, atoms on the "bottom" of the molecule ("below" the Zr_4 plane) are labeled with a prime and those related by inversion symmetry on the "top" of the molecule ("above" the Zr_4 plane) are labeled without a prime. The two "surfaces" of the metal−oxygen core are layers of approximately closest packed oxygen atoms. These two layers are stacked in ap-

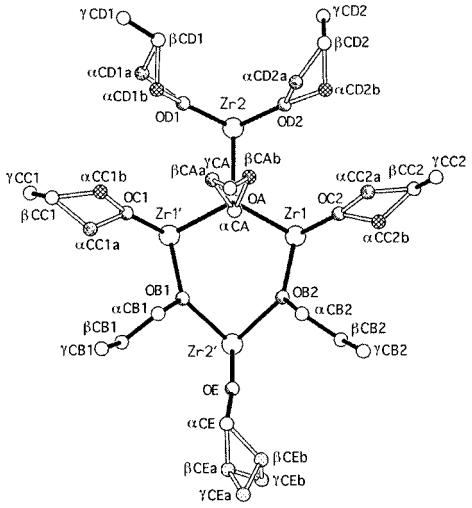

Figure 2. Asymmetric unit of the $Zr_4(OPr^n)_{16}$ molecule in the solid state. Ordered zirconium, oxygen, and carbon atoms are represented by large, unshaded; small, shadowed; and small, unshaded spheres, respectively. Alternate positions for carbon atoms are represented by cross-hatched, small spheres; speckled, small spheres; and regularly dotted, small spheres. Hydrogen atoms have been omitted for clarity. Bonds from disordered carbon atoms to other atoms are represented by hollow bonds.

proximately closest packing, and the zirconium atoms occupy octahedral interstices between the layers. When idealized C_{2h} symmetry is assumed, two types of Zr centers, labeled Zr1 and Zr2 in Figure 1, and five types of *n*-propoxide oxygen atoms, labeled OA through OE in Figure 1, are obtained. The ZrO_6 zirconium coordination polyhedra are approximately octahedral, and each metal center is displaced from the center of its coordination polyhedron such that Zr−O bonds to terminal alkoxide ligands are relatively short, averaging 1.94(1,2,2,5) Å,[41] and Zr−O bonds to bridging alkoxide ligands are relatively long, averaging 2.17(1,7,10,3) and 2.33(1,1,2,3) Å for doubly and triply bridging ligands, respectively.

All of the non-hydrogen atoms in the asymmetric unit of $Zr_4(OPr^n)_{16}$ are shown in Figure 2, where two symmetry-related Zr atoms are included for purposes of clarity. Only the type B, doubly bridging *n*-propoxide ligands are ordered. The remaining *n*-propoxide ligands contain at least one disordered carbon atom as indicated in Figure 2, where bonds to disordered carbon atoms are represented by hollow lines. By examining carbon−carbon contacts in the disordered centrosymmetric structure of **1**, two, and only two, alternative ligand conformations can be identified for the type A, C, and D *n*-propoxide ligands in which all nonbonding carbon−carbon separations less than the 3.40 Å[42] van der Waals diameter of carbon are avoided.[43] These two conformations are identified in Figure 2, where carbon atoms in conformation a are represented by shaded spheres and carbon atoms in conformation b are represented by crosshatched spheres. In Figure 3, where γ-methyl groups have been omitted for purposes of clarity, conformations a and b are shown in space-filling representations. The doubly bridging, type B

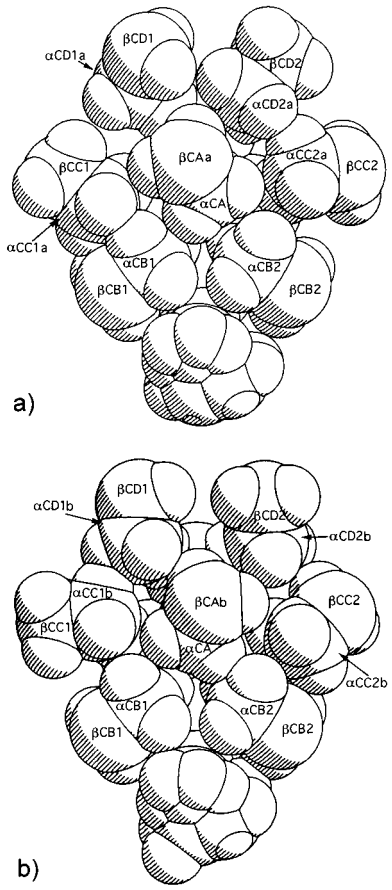

Figure 3. Space-filling representations of (a) the "top" surface (conformation a) and (b) the "bottom" surface (conformation b) of the $Zr_4(OPr^n)_{16}$ molecule. All γ-methyl groups have been omitted for purposes of clarity. In both drawings, C−H bond lengths of 1.09 Å and experimentally determined C−C and C−O bond lengths were employed. Spheres representing these atoms have van der Waals radii of 1.7, 1.4, and 1.2 Å for C, O, and H, respectively.

alkoxide ligands adopt the rotameric conformation about their carbon−oxygen bonds expected on steric grounds,[44] and the triply bridging, type A alkoxide ligands adopt "clockwise" (conformation b) and "counterclockwise" (conformation a) carbon−oxygen rotameric conformations that avoid repulsive interactions with the type B, doubly bridging alkoxide ligands.[45] Both conformations are combined in Figure 4, one on the "top" surface of the molecule (conformation a) and the other on the "bottom" surface (conformation b). The particular combination of conformations shown in Figure 4 is arbitrary, since there are no <3.40 Å intra- or intermolecular C···C contacts between carbon atoms in type A−D *n*-propoxide groups on the "top" and carbon atoms in type A−D *n*-propoxide groups on the "bottom" of the molecule that might suggest an energetic preference. All of the alternative positions for disordered carbon atoms in the type E *n*-propoxide groups are shown in Figures 2−4, since none of the possible alternative *n*-propyl conformations imply inter- or intramolecular nonbonding carbon−carbon distances shorter than 3.40 Å. Note that the crystallographic data do not allow for a distinction between dynamic and static disorder.

(41) The first number in parentheses following an average value of a bond length or interatomic distance is the root-mean-square estimated standard deviation of an individual datum. The second and third numbers are the average and maximum deviations from the average value, respectively. The fourth number represents the number of individual measurements which are included in the average value.

(42) Pauling, L. *The Nature of the Chemical Bond*; Cornell University Press: Ithaca, NY, 1960; p 260.

(43) The C···C separations are βCAa···αCC1b = 3.36 Å, βCAa···αCD1b = 3.20 Å, βCAb···αCD2a = 3.21 Å, and αCC2a···αCD2b = 3.26 Å.

(44) Day, V. W.; Klemperer, W. G.; Schwartz, C. *J. Am. Chem. Soc.* **1987**, *109*, 6030−6043.

(45) The same conformation is observed for triply bridging ethoxide groups in $W_4(OEt)_{16}$: Chisholm, M. H.; Huffman, J. C.; Kirkpatrick, C. C.; Leonelli, J.; Folting, K. *J. Am. Chem. Soc.* **1981**, *103*, 6093−6099.

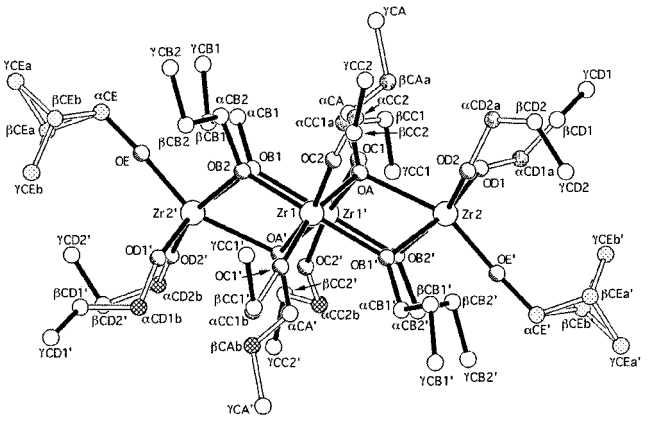

Figure 4. Perspective drawing of a hypothetical, ordered $Zr_4(OPr^n)_{16}$ molecule in the solid state. All hydrogen atoms have been omitted for purposes of clarity, and all other atoms are represented as in Figure 2. Atoms labeled with a prime are related to atoms in the asymmetric unit labeled without a prime by the crystallographic inversion center located at (1/2, 0, 1/2) in the unit cell of the centrosymmetric space group used for structure refinement of the disordered structure.

^{13}C{^{1}H} Solution NMR Spectroscopy. Solution ^{13}C{^{1}H} 188.6 MHz NMR spectra of tetra-*n*-propyl zirconate measured at −20 °C display five resonances in each of the three *n*-propyl carbon regions (see Figure 5b−d). Relative intensities of 1:1:2:2:2 (a:e:b:c:d when labeled as in Figure 5b−d) are obtained in each region when spectra are measured using gated decoupling, and these ratios are consistent with a C_{2h} $Zr_4(OPr^n)_{16}$ structure having the same Zr_4O_{16} core structure observed for tetra-*n*-propyl zirconate in the solid state (see Figure 1). As shown in Figure 5a, for the alkoxide oxygen atoms, this C_{2h} idealized core structure contains two type A and two type E *n*-propoxide groups and four each of the remaining type B, C, and D *n*-propoxide groups. Resonances labeled with the same lowercase letters in Figure 5b−d were assigned to the same *n*-propoxide group as follows: Spin−spin coupling between α-methylene and *β*-methylene protons and between *β*-methylene and *γ*-methyl protons in each of the five types of propyl groups was identified using two-dimensional gradient-enhanced ^{1}H−^{1}H COSY spectroscopy at 750 MHz. Each set of three coupled proton resonances identified with a given type of propyl group was then associated with a unique set of three carbon resonances from heteronuclear ^{1}H, ^{13}C chemical shift correlations obtained using gradient phase-sensitive ^{1}H−^{13}C HMQC spectroscopy. In this fashion, the sets of low-intensity resonances a and e were collectively assigned to *n*-propoxide groups A and E, and the sets of high-intensity resonances b, c, and d were collectively assigned to *n*-propoxide groups B, C, and D.

A more complete assignment of ^{13}C resonances was obtained from ^{13}C longitudinal relaxation times (T_1) measured at −11 °C. The relaxation times observed for α-methylene, *β*-methylene, and *γ*-methyl carbon resonances are displayed graphically in Figure 6. Noting that ln T_1 vs $1/T$ plots for *β*-methylene and *γ*-methyl carbon nuclei are linear between +25 and −11 °C[40] and making the assumption that relaxation times for ^{13}C resonances assigned to "anchored" hydrocarbon chains in fluid solution are governed by dipole−dipole interactions in the extreme narrowing limit,[46−48] relaxation times T_1 are expected to vary inversely with rotational correlation time (τ_C) such that

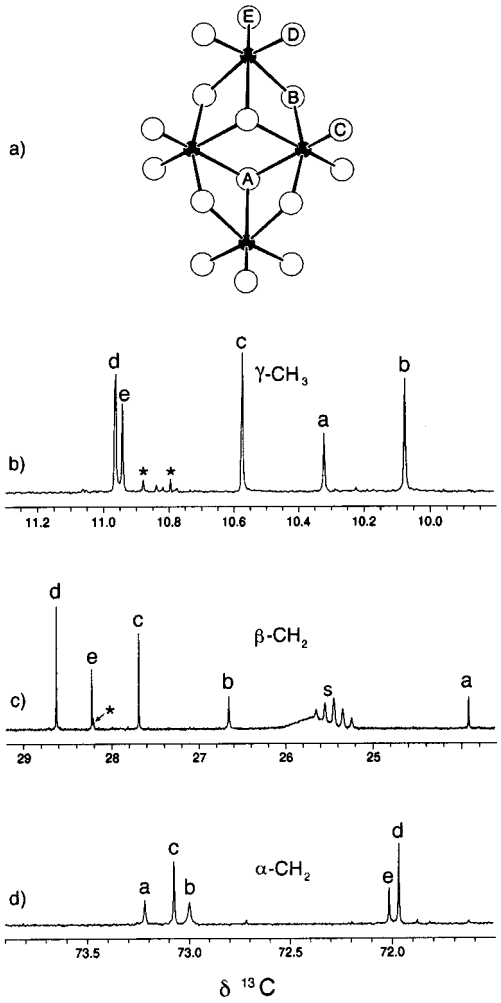

Figure 5. Zr_4O_{16} metal−oxygen framework of $Zr_4(OPr^n)_{16}$ (a). Zirconium atoms are represented by small, filled spheres, and oxygen atoms are represented by large, open spheres. One member of each symmetry-equivalent set of alkoxide oxygen atoms is labeled assuming C_{2h} symmetry. The 188.6 MHz ^{13}C{^{1}H} NMR spectrum of $Zr_4(OPr^n)_{16}$ in methylcyclohexane-d_{14} solution at −20 °C in the *γ*-methyl (b), *β*-methylene (c), and α-methylene (d) chemical shift regions. The solvent resonance band is labeled with an "s"; resonances assigned to $Zr_3O(OPr^n)_{10}$ are labeled with asterisks.

longer relaxation times reflect greater mobility. For each of the five different types of *n*-propyl groups, the α-methylene carbon resonance has the shortest T_1 value and the *γ*-methyl carbon resonance has the longest T_1 value, which is the anticipated relationship since α-methylene carbon atoms are anchored directly to the metal oxide framework while *γ*-methyl carbon atoms are most remote from the anchor point. Comparison of relaxation times for a given type of carbon atom (α, *β*, or *γ*) in the different *n*-propyl groups reveals in each case significantly shorter relaxation times for ^{13}C nuclei associated with resonances a and b relative to relaxation times for ^{13}C nuclei associated with resonances c, d, and e, implying significantly lower mobility for two types of *n*-propyl groups relative to the other three. Given the conformational constraints placed on α-methylene carbon atoms bonded to bridging oxygen atoms relative to α-methylene carbon atoms bonded to terminal oxygen atoms (see above), shorter relaxation times are anticipated for bridging *n*-propoxide groups relative to terminal *n*-propoxide groups,

(46) Breitmaier, E.; Voelter, W. *^{13}C NMR Spectroscopy. Methods and Applications in Organic Chemistry*; Verlag Chemie: New York, 1978; pp 110−129.
(47) Wehrli, F. W.; Wirthlin, T. *Interpretation of Carbon-13 NMR Spectra*; Heyden: London, 1978; pp 129−151.
(48) Lyerla, J. R., Jr.; Levy, G. C. In *Topics in Carbon-13 NMR Spectroscopy*; Levy, G. C., Ed.; Wiley: New York, 1974; Vol. 1, pp 79−148.

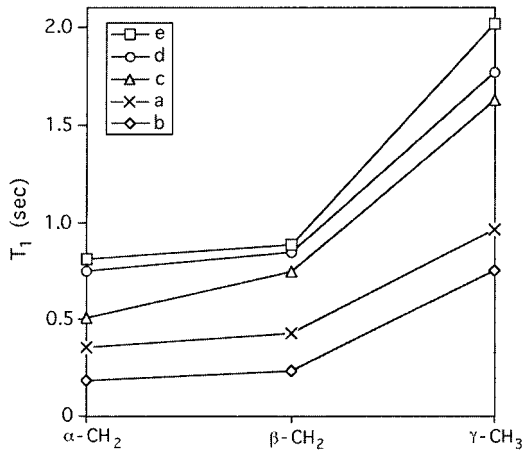

Figure 6. Longitudinal relaxation times (T_1) at −11 °C for α-methylene, β-methylene, and γ-methyl ^{13}C nuclei in $Zr_4(OPr^n)_{16}$ measured in methylcyclohexane-d_{14} solution at 188.6 MHz.

implying assignment of resonances a and b to the two types of bridging *n*-propoxide groups and methyl resonances c, d, and e to the three types of terminal *n*-propoxide groups. When combined with assignments made above based on intensity arguments, ^{13}C longitudinal relaxation times imply assignment of resonances labeled a, b, and e in Figure 5b−d to type A, B, and E *n*-propoxide groups, respectively, as labeled in Figure 5a. Only resonances c and d remain to be assigned to terminal *n*-propoxide groups C and D (or D and C). Since relaxation times associated with resonances c are consistently shorter than relaxation times associated with resonances d for each type of carbon atom (see Figure 6), type C and D *n*-propoxide groups clearly have different mobilities. In the solid state, type C *n*-propyl groups are less sterically encumbered than type D *n*-propyl groups: of the six C···C nonbonded distances shorter than 3.65 Å in crystalline $Zr_4(OPr^n)_{16}$,[49] one involves a type A *n*-propyl group, six involve type B *n*-propyl groups, five involve type C *n*-propyl groups, one involves a type D *n*-propyl group, and none involve type E *n*-propyl groups. In the solid state, type C *n*-propyl groups are in this respect the most confined terminal *n*-propyl groups and presumably the least mobile. Assuming the same pattern of behavior in solution, resonances c and d may be assigned to *n*-propyl groups C and D, respectively.

Discussion

Isolation of $Zr(OPr^n)_4$. Tetra-*n*-propyl zirconate was first prepared as an impure dark brown solid by Bradley and Wardlaw by allowing $ZrCl_4$ to react with 1-propanol in the presence of ammonia.[11] Bradley et al. later reported that analytically pure $Zr(OPr^n)_4$ could be obtained as a highly viscous liquid with a boiling point of 208 °C (0.1 mmHg) by alkoxide exchange of tetraisopropyl zirconate with 1-propanol.[12] In subsequent thermal stability studies,[8,9] Bradley and co-workers demonstrated that zirconium alkoxides containing β-hydrogen atoms undergo facile decomposition at elevated temperatures (see eq 1), a reasonable result given the known moisture sensitivity of zirconium alkoxides and the known catalytic activity of ZrO_2 for alcohol dehydration.[7a,c,50,51] Furthermore, they observed that alkoxide decomposition could be minimized during fractional distillation by prior removal of alcohol from the system. In the present study, $Zr(OPr^n)_4$ was purified as prescribed by Bradley et al., but the fractional distillation was performed at lower pressure, ca. 10^{-2} mmHg. The first distillation fraction, a highly viscous liquid at ambient temperature and pressure, was collected between 185 and 220 °C, and the amount of material collected was dependent upon the purity of the crude material, relatively pure starting material yielding a relatively small first fraction. This fraction, containing both tetra-*n*-propyl zirconate and its hydrolysis product $Zr_3O(OPr^n)_{10}$,[52] appears to be the liquid reported by Bradley et al.[12] The second distillation fraction, collected between 225 and 245 °C, was analytically pure $Zr_4(OPr^n)_{16}$, a white solid at ambient temperature and pressure.

The inability to isolate very reactive metal alkoxides is well-documented not only for zirconium and hafnium alkoxides[13,14] but also for scandium, yttrium, indium, and ytterbium alkoxides.[53] The present study illustrates, however, that, in the case of zirconium *n*-propoxide, very reactive alkoxides can be obtained in pure form, but only if extreme measures are taken, namely, distillation at low pressure and high temperature over a short time period. It is not unlikely that this approach can be extended to other systems, and the importance of this possibility cannot be underestimated, given that the most chemically reactive alkoxides are in many respects the most attractive and interesting alkoxides.

Structures of $Zr_4(OPr^n)_{16}$ and $[CH_3C(CH_2O)_3]_2Zr_4(OPr^i)_{10}$. The $Zr_4(OPr^n)_{16}$ molecule (**1**) has the metal−oxygen core structure **a,** as is the case for $Ti_4(OCH_2CH_3)_{16}$,[21] $Ti_4(OCH_3)_4(OCH_2CH_3)_{12}$,[22] $Ti_4(OCH_3)_{16}$,[23] $[CH_3C(CH_2O)_3]_2Ti_4(OPr^i)_{10}$ (**2**),[19] and $[CH_3CH_2C(CH_2O)_3]_2Ti_4(OPr^i)_{10}$ (**3**),[19] but *not* the case for $[CH_3C(CH_2O)_3]_2Zr_4(OPr^i)_{10}$ (**4**),[19] which has the metal−oxygen core structure **b**. The structure observed for **4** is therefore not characteristic of tetrameric alkyl orthozirconates in general, raising the question why structure **b** is observed for **4** when structure **a** is observed for the other orthotitanates and -zirconates just enumerated. Before discussion of the specific factors responsible for this difference in structure, it should first be noted that the zirconium centers in **1**, unlike the titanium centers in its orthotitanate analogues, are coordinatively unsaturated and therefore susceptible to distortion of their octahedral coordination polyhedra toward trigonal prismatic coordination as observed in **4**. The average O···O contact distance for ZrO_6 coordination polyhedra in **1** is 2.96 Å, a value significantly greater than the 2.8 Å van der Waals diameter of oxygen.[42] In contrast, the average O···O contact distance for TiO_6 coordination polyhedra in $Ti_4(OCH_3)_{16}$ is 2.80 Å.[23] The octahedral coordination polyhedra in **1** may therefore distort toward trigonal metaprismatic geometry without increasing zirconium−oxygen

(49) The C···C separations are αCC1a···βCB1 = 3.38 Å, αCA···αCB2 = 3.57 Å, αCD1b···αCC1b = 3.39 Å, αCC2b···αCB2 = 3.47 Å, αCC2b···βCB2′ = 3.57 Å, and αCC1a···αCB1′ = 3.14 Å.

(50) Yamaguchi, T.; Sasaki, H.; Tanabe, K. *Chem. Lett.* **1973**, 1017−1018 and references therein.

(51) Zechmann, C. A.; Folting, K.; Caulton, K. G. *Chem. Mater.* **1998**, *10*, 2348−2357.

(52) At ambient temperature, 125.6 MHz $^{13}C\{^1H\}$ NMR spectra measured from cyclohexane-d_{12} solutions display $Zr_4(OPr^n)_{16}$ resonances (see the Experimental Section) and additional resonances at δ 73.13, 72.30, 28.47, 10.87, and 10.83 assigned to $Zr_3O(OPr^n)_{10}$.[14,40] Other resonances were observed at δ 78.09, 77.96, 73.42, 28.14, 28.12, 27.32, 10.83, and 10.61 which could not be assigned to either $Zr_4(OPr^n)_{16}$ or $Zr_3O(OPr^n)_{10}$.

(53) (a) Bradley, D. C.; Chudzynska, H.; Frigo, D. M.; Hammond, M. E.; Hursthouse, M. B.; Mazid, M. A. *Polyhedron* **1990**, *9*, 719−726. (b) Mazdiyasni, K. S.; Lynch, C. T.; Smith, J. S. *Inorg. Chem.* **1966**, *5*, 342−346. (c) Brown, L. M.; Mazdiyasni, K. S. *Inorg. Chem.* **1970**, *9*, 2783−2786. (d) Evans, W. J.; Meadows, J. H.; Kostka, A. G.; Closs, G. L. *Organometallics* **1985**, *4*, 324−326. (e) Poncelet, O.; Sartain, W. J.; Hubert-Pfalzgraf, L. G.; Folting, K.; Caulton, K. G. *Inorg. Chem.* **1989**, *28*, 263−267. (f) Page, C. J.; Sur, S. K.; Lonergan, M. C.; Parashar, G. K. *Magn. Reson. Chem.* **1991**, *29*, 1191−1195.

bond lengths or decreasing the average O···O separation below 2.8 Å, whereas titanium centers in **2** may undergo this distortion only at the energetic expense of increasing metal−oxygen bond lengths and/or decreasing the average O···O contacts below 2.8 Å. Consider, for example, the extreme case of rigorously trigonal prismatic MO_6 coordination, where the O_6 coordination polyhedron has equilateral square and triangular faces. Radius ratio calculations dictate that 2.8 Å O···O contacts imply 2.14 Å M−O bond distances, a distance significantly longer the 1.98 Å average Ti−O bond length in **2** and **3**, but only slightly longer than the 2.11 Å average Zr−O bond distance observed for **1**. On the other hand, radius ratio calculations for rigorously trigonal prismatic MO_6 coordination with 2.0 Å M−O bond distances implies very short, 2.6 Å O···O contacts.

Where accurate metric data are available,[19] comparison of interatomic distances in molecule **1** and titanium alkoxides having the same metal−oxygen core structure reveals systematic differences (see Table 2). The difference in average bond length for each type of metal−oxygen bond closely approximates the 0.11−0.15 Å difference between the radii of Zr and Ti.[54] A slightly larger, about 0.20 Å average difference between oxygen−oxygen separations in the ZrO_6 and TiO_6 octahedral coordination polyhedra and a far greater difference of 0.29−0.56 Å between metal−metal separations is also evident (see Table 2). Overall, the dimensions of the Zr_4O_{16} oxide core structure in **1** are 5−10% greater than the dimensions of the Ti_4O_{16} oxide core structure in **2** and **3**. This difference in size has two important implications concerning the relative compatibilities of different organic groups with the M_4O_{16} core structure **a**.

The larger dimensions of the M_4O_{16} oxide core structure **a** in **1** relative to the dimensions of its orthotitanate analogues imply greater compatibility with relatively large alkyl groups bonded to its surface. In this context, note that although $Ti_4(OCH_3)_{16}$, like $Zr_4(OPr^n)_{16}$, is stable toward dissociation in saturated hydrocarbon solution at ambient temperature, its tetrameric ethyl analogue dissociates under the same conditions.[60,61] This instability can be rationalized in terms of greater steric repulsion between alkyl groups bonded to the smaller Ti_4O_{16} orthotitanate core.

The smaller dimensions of the M_4O_{16} oxide core structure **a** in alkyl orthotitanates relative to the dimensions of their zirconium analogue imply greater compatibility with chelating ligands having relatively small bite sizes. The bite size of the $CH_3C(CH_2O)_3$ ligand is 2.7−2.8 Å,[62−64] a distance clearly

Chart 1

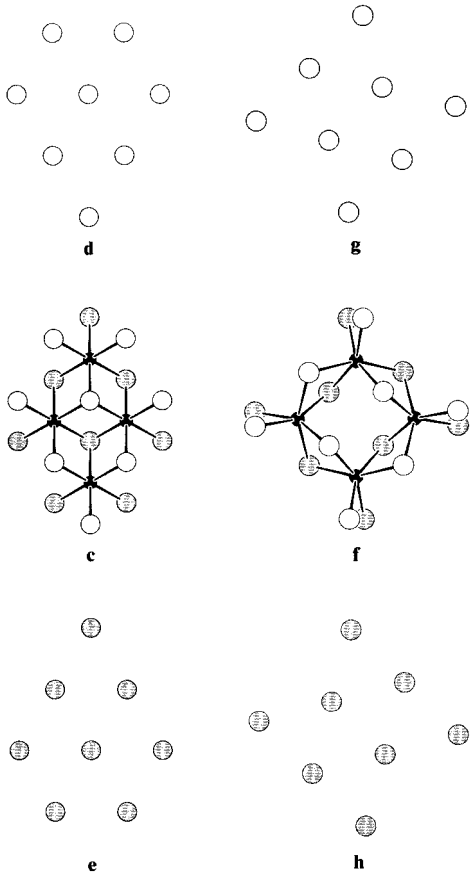

compatible with the 2.74−2.91 Å O···O separations between the corresponding oxygen atoms in $Ti_4(OCH_3)_{16}$ (see shaded spheres in **a**), such that titanates **2** and **3** adopt core structure **a** with 2.69−2.82 Å O···O separations between the oxygen atoms in each chelate ligand. However, the bite size of the tridentate chelating ligand is apparently incompatible with the 2.92−3.18 Å O···O separations between the relevant oxygens in **1**: binding two $CH_3C(CH_2)_3$ groups to the Zr_4O_{16} oxide core structure observed for **1** would impose an energetically unfavorable geometry on the $CH_3C(CH_2O)_3$ ligand. If, however, the geometry of the distorted chelate ligand in this hypothetical molecule were relaxed to obtain a 2.78−2.85 Å bite size as observed in **4**, some of the bonds from zirconium atoms to the six oxygen atoms involved would be stretched significantly. This incompatibility is resolved by distortion of the Zr_4O_{16} geometry from **a** into **b**, where the square arrangement of Zr centers allows for short O···O separations in the chelate ligands, 2.78−2.83 Å in **4**, while maintaining appropriately short Zr−O bond distances (the average Zr−O bond distance in **4** is 2.09 Å). From an energetic point of view, the key difference between the Zr_4O_{16} oxide core structure **a** observed for **1** and the Zr_4O_{16} oxide core structure **b** observed for **4** therefore appears not to be metal coordination geometry but metal−metal separation. If molecule **4** were required to adopt the approximately C_{2h} Zr_4O_{16} oxide core structure observed for $Zr_4(OPr^n)_{16}$ (**1**), the $CH_3C(CH_2O)_3$ ligands would be required to span metals separated by 6.25 Å, namely, the Zr2···Zr2′ separation in **1** (see Figures 1 and 4 and Table 2). By adopting the approximately D_{2d} M_4O_{16} structure **b**, the $CH_3C(CH_2O)_3$ ligands are required to chelate metals separated by only 3.49−5.03 Å in **4**.

The M_4O_{16} structure **b** has been treated thus far as a distorted version of structure **a**, and although this is the case locally in terms of metal coordination geometry, it is not the case globally

(54) The radii of zirconium and titanium, respectively, are 1.55 and 1.40 Å as Slater−Bragg radii,[55] 0.86 and 0.745 Å as Shannon and Prewitt ionic radii[56] for coordination number 6, 0.77 and 0.64 Å as Goldschmidt ionic radii,[57] 0.79 and 0.68 Å as Ahrens ionic radii,[57] 1.454 and 1.324 Å as Pauling single-bond metallic radii,[58] 0.80 and 0.68 Å as Pauling crystal radii,[59] and 1.09 and 0.96 Å as Pauling univalent radii.[59]

(55) Slater, J. C. *Quantum Theory of Molecules and Solids*; MgGraw-Hill: New York, 1965; Vol. 2, p 55.
(56) Shannon, R. D. *Acta Crystallogr.* **1976**, *A32*, 751−767.
(57) Megaw, H. D. *Crystal Structure: A Working Approach*; Saunders: Philadelphia, 1973; pp 26−27.
(58) Pauling, L. *The Nature of the Chemical Bond*; Cornell University Press: Ithaca, NY, 1960; p 256.
(59) Pauling, L. *The Nature of the Chemical Bond*; Cornell University Press: Ithaca, NY, 1960; p 514.
(60) Weingarten, H.; Van Wazer, J. R. *J. Am. Chem. Soc.* **1965**, *87*, 724−730.
(61) Bradley, D. C.; Holloway, C. E. *J. Chem. Soc. A* **1968**, 1316−1319.
(62) Liu, S.; Ma, D.; McGowty, D.; Zubieta, J. *Polyhedron* **1990**, *9*, 1541−1553.
(63) Ma, L.; Liu, S.; Zubieta, J. *Inorg. Chem.* **1989**, *28*, 175−177.
(64) Wilson, A. J.; Robinson, W. T.; Wilkins, C. J. *Acta Crystallogr.* **1983**, *C39*, 54−56.

with regard to the entire metal−oxygen framework. In an idealized version of structure **a**, four metal atoms are sandwiched between two identical, parallel layers of eight closest packed oxygen atoms, one layer represented by shaded large spheres and the other layer represented by unshaded large spheres in **c** (see Chart 1). These two layers are oriented such that rows of closest packed oxygen atoms in one layer are parallel to rows of closest packed oxygen atoms in the other layer (see **d** and **e** in Chart 1) and are aligned such that each of the four metal centers has perfectly octahedral coordination geometry (see **c**) and C_{2h} molecular symmetry is obtained. Structure **b** very closely approximates the idealized structure **f** shown in Chart 1 where four metal atoms are sandwiched between two parallel layers of eight closest packed oxygen atoms, one layer represented by large shaded spheres and the other layer by large unshaded spheres. These layers are oriented such that rows of closest packed oxygen atoms in one layer are perpendicular to rows of closest packed oxygen atoms in the other layer (see **g** and **h** in Chart 1) and D_{2d} molecular symmetry is obtained (see **f**). Since D_{2d} is not a subgroup of C_{2h}, structure **f** is not a distorted version of structure **c**. In terms of local metal coordination geometry, however, structure **f** (idealized **b**) is a distorted version of **c** (idealized **a**), since metal coordination polyhedra in **f** have only C_2 symmetry whereas the metal coordination geometry is rigorously octahedral in **c**. For an alternative perspective on the structural relationships just described, see the cover art for this issue [*Inorg. Chem.* **2001**, *40* (23)], where real, not idealized, structures are shown.

Acknowledgment. W.G.K. is grateful to Don Bradley for teaching him the important basics of zirconium alkoxide chemistry. W.G.K. and M.M.P. are grateful to Peter Petillo for helpful discussions on longitudinal relaxation times. Support by the Department of Energy Grant DE-FG02-91ER45349 through the Frederick Seitz Materials Research Laboratory at the University of Illinois is gratefully acknowledged. NMR spectra were obtained in the Varian Oxford Center for Excellence in NMR Laboratory. Funding for this instrumentation was provided in part from the W. M. Keck Foundation, the National Institutes of Health (Grant PHS 1 S10 RR10444-01), and the National Science Foundation (NSF; Grant CHE 96-10502). The cover graphic was supplied by Glenn Westwood and Jim Goloboy.

Supporting Information Available: Crystal structure analysis report, tables of atomic coordinates for non-hydrogen atoms, anisotropic thermal parameters for non-hydrogen atoms, atomic coordinates for hydrogen atoms, bond lengths, and bond angles, perspective drawings of the disordered solid-state structure using spheres and using 30% probability thermal vibration ellipsoids, and CIF files for $Zr_4(OPr^n)_{16}$. This material is available free of charge via the Internet at http://pubs.acs.org.

IC010776G